Metabolic engineering of Synechocystis sp. PCC 6803 for the production of aromatic amino acids and derived phenylpropanoids

Brey, Laura Furelos; Wodarczyk, Artur J.; Bang Thøfner, Jens F.; Burow, Meike; Crocoll, Christoph; Nielsen, Isabella; Zygadlo Nielsen, Agnieszka J.; Jensen, Poul Erik

Published in:
Metabolic Engineering

DOI:
10.1016/j.ymben.2019.11.002

Publication date:
2020

Document version
Publisher's PDF, also known as Version of record

Metabolic Engineering 57 (2020) 129–139

Contents lists available at ScienceDirect

Metabolic Engineering

journal homepage: www.elsevier.com/locate/meteng

Metabolic engineering of *Synechocystis* sp. PCC 6803 for the production of aromatic amino acids and derived phenylpropanoids

Laura Furelos Brey[a], Artur J. Włodarczyk[b], Jens F. Bang Thøfner[a], Meike Burow[a,c], Christoph Crocoll[a,c], Isabella Nielsen[a], Agnieszka J. Zygadlo Nielsen[a], Poul Erik Jensen[a,*,1]

[a] *Copenhagen Plant Science Center, Department of Plant and Environmental Sciences, University of Copenhagen, Thorvaldsensvej 40, DK-1871, Frederiksberg C, Copenhagen, Denmark*

[b] *School of Biological Sciences, Nanyang Technological University, 60 Nanyang Drive, 637551, Singapore*

[c] *DynaMo Center, Department of Plant and Environmental Sciences, University of Copenhagen, Thorvaldsensvej 40, DK-1871, Frederiksberg C, Copenhagen, Denmark*

A B S T R A C T

In light of the climate change challenge, the advantageous trait of using solar energy and carbon dioxide to produce organic molecules has granted cyanobacteria deserved interest as hosts for metabolic engineering. Importantly, these organisms do not directly compete with agricultural resources. Aromatic amino acids and derived phenylpropanoids are of high importance because they are used by the pharmaceutical, food, cosmetic, and agricultural industries as precursors of active ingredients. Amino acids are traditionally produced by extraction from protein hydrolysates, chemical synthesis or fermentation pathways using heterotrophic microorganisms. In this work we demonstrate for the first time the efficient overproduction of phenylalanine and tyrosine from CO_2 in a *Synechocystis* sp. PCC 6803 strain heterologously expressing the feedback-inhibition-resistant AroG and TyrA enzymes from *E. coli*. Production titers reached 904 ± 53 mg/gDW (580 ± 34 mg/L) of phenylalanine and 64 ± 3.7 mg/gDW (41 ± 2.3 mg/L) of tyrosine after 10 days of photoautotrophic growth. We estimate that the production of the two amino acids corresponds to 56% of the total fixed carbon. Phenylalanine and tyrosine are the precursors for phenylpropanoids, thus, we tested the functionality of several phenylpropanoid biosynthetic enzymes in the generated cyanobacterium strains and successfully achieved the production of 470 ± 70 mg/gDW (207 mg/L) of *p*-coumaric acid, 267 ± 31 mg/gDW (114 mg/L) of cinnamic acid and 47.4 ± 13.9 mg/gDW (12.6 mg/L) of caffeic acid after 6 days of photoautotrophic growth. All compounds were secreted to the growth medium. Our work enlarges the repertoire and yield of heterologous chemicals produced by *Synechocystis* and contributes to extend the molecular knowledge about this cyanobacterium.

1. Introduction

The aromatic amino acids (AAAs): L-phenylalanine (phenylalanine), L-tyrosine (tyrosine) and L-tryptophan (tryptophan), are of commercial interest because of their broad applicability in the food, pharmaceutical and chemical industries. For example, phenylalanine is used as precursor of the artificial sweetener aspartame, whereas tyrosine is used as precursor of the anti-Parkinson drug L-DOPA (Rodriguez et al., 2014). Additionally, AAAs are the precursors of highly demanded natural products such as phenylpropanoids and derived flavonoids (Pietta et al., 2000). Historically, the AAAs have been produced through chemical synthesis, however this is a disadvantageous approach because it employs non-renewable toxic raw materials and generates mixtures of D and L isomers which are difficult to purify. After years of research *E. coli* has been successfully engineered in a number of ways to overproduce AAAs and several derived aromatic acids (Rodriguez et al., 2014). The biotechnological production of AAA and phenylpropanoids in cyanobacteria would present an environmental advantage over traditional heterotrophic hosts like *E. coli*, as cyanobacteria being photosynthetic organisms do not depend on carbohydrate resources from arable land. Among all cyanobacteria species, *Synechocystis* sp. PCC 6803 (hereafter *Synechocystis*) is a model organism for photosynthetic studies (Berla et al., 2013). Recently it has been shown that *Synechocystis* can successfully be used to express P450-dependent pathways and that produced metabolites are readily secreted to the growth media which facilitates product recovery (Wlodarczyk et al., 2016). Importantly, metabolic profiling of *Synechocystis* showed that the internal pools of AAAs in this species are amongst the highest for cyanobacteria regularly used as chassis for metabolic engineering (Dempo et al., 2014). Therefore, *Synechocystis* is a good candidate for sustainable AAAs overproduction.

All three AAAs are produced from the common precursor chorismate synthesized through the Shikimate pathway (Fig. 1). The Shikimate pathway starts with the condensation of phosphoenolpyruvate (PEP) and erythrose-4-phosphate (E4P) to form 3-deoxy-D-arabino-heptulosonate-7-phosphate (DAHP). This reaction is catalyzed by the

* Corresponding author. University of Copenhagen, Rolighedsvej 26, DK-1958, Frederiksberg, Denmark.
E-mail address: peje@food.ku.dk (P.E. Jensen).
[1] Current address: Department of Food Science, University of Copenhagen, Rolighedsvej 26, DK-1958, Frederiksberg.

https://doi.org/10.1016/j.ymben.2019.11.002
Received 1 August 2019; Received in revised form 14 October 2019; Accepted 8 November 2019
Available online 10 November 2019

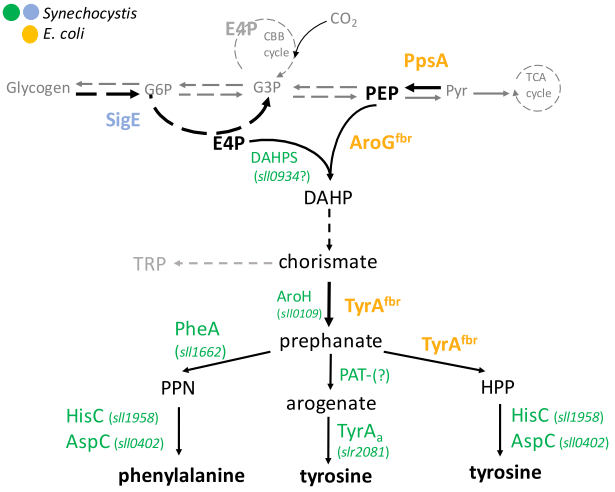

Fig. 1. Schematic representation of the phenylalanine and tyrosine biosynthetic pathways in *Synechocystis* as annotated in the Kyoto Encyclopedia of Genes and Genomes (KEGG). In green, the predicted biosynthetic enzymes and coding loci from *Synechocystis* as annotated in KEGG. In orange the *E. coli* enzymes introduced in *Synechocystis* to attempt AAA overproduction in this work. In blue *Synechocystis* SigE Group 2 sigma factor used in this work to activate the transcription of several sugar catabolic genes and increase the precursor E4P (erythrose-4-phosphate). Question marks illustrate loci that have either not been predicted yet or that have been predicted but there is contradicting experimental data. Abbreviations: TCA tricarboxylic acid cycle, TRP tryptophan, PEP phosphoenolpyruvate, E4P erythrose-4-phosphate, DAHP 3-Deoxy-D-arabino-heptulosonate-7-phosphate, PPN phenylpyruvate, HPP 4-hydroxyphenylpyruvate, PAT prephanate amino transferase, G6P glucose-6-phospate, G3P glyceraldehyde-3-phosphate, Pyr pyruvate. . (For interpretation of the references to color in this figure legend, the reader is referred to the Web version of this article.)

DAHP synthase (DAHPS) enzyme and it is the most tightly regulated step in the pathway (Mir et al., 2015). In bacteria, carbon flow through the pathway is mostly regulated by feedback inhibition of DAHPS (Entus et al., 2002). In *E. coli* three different DAHPS isoforms are known, namely AroG, AroF and AroH, which are feedback-inhibited by phenylalanine, tyrosine and tryptophan, respectively (Brown et al., 1966). Eighty percent of the DAHP synthase activity in *E. coli* has been attributed to the AroG isoform (Jensen et al., 1968). In *E. coli* the amino acid residues responsible for the feedback inhibition sensitivity of each DAHPS isoform have been identified and mutated, resulting in feedback resistant DAHPS versions (Kikuchi et al., 1997). To date, the DAHPS from *Synechocystis* remain unidentified, and only the *sll0934* locus has been predicted to encode one single DAHPS (Kyoto Encyclopedia of Genes and Genomes (KEGG); https://www.genome.jp/kegg/}). However, *sll0*934 has also been annotated as a carboxysome formation protein and experimental data from Ogawa et al. (1994) shows that full segregation of a knock out mutant is possible, suggesting the existence of alternative DAHP synthases. Although the biochemical regulation of DAHP synthases in *Synechocystis* has never been studied, data on the enzymatic activity of DAHPS from the closely related *Synechocystis* sp. PCC 6714 strain revealed potent inhibition by phenylalanine (Hall et al., 1982), suggesting that feedback-inhibition of DAHPS could also exist in *Synechocystis*.

After chorismate, the pathway branches into the terminal AAA-specific biosynthetic pathways: it can be used to synthesize tryptophan, or it can be isomerized to prephanate for phenylalanine and tyrosine synthesis (Fig. 1). Cyanobacteria have diverse phenylalanine and tyrosine biosynthetic pathways (Hall et al., 1982), which have been less characterized and differ slightly from those in *E. coli*. Whereas in *Synechocystis* the synthesis of phenylalanine has been predicted to occur like in *E. coli* through the activity of the prephanate dehydratase PheA enzyme, the synthesis of tyrosine is known to occur via arogenate like in plants: prephanate undergoes direct transamination to arogenate, by a yet unidentified prephanate aminotransferase (PAT), and it is then dehydrogenated and decarboxylated to tyrosine by $TyrA_a$ (Fig. 1). Unlike PheA, whose coding gene and activity has only been predicted by homology in *Synechocystis*, $TyrA_a$, encoded by the *slr2081* locus has been purified, crystalized and thoroughly characterized (Bonner et al., 2004; Legrand et al., 2006). The dehydrogenase activity of $TyrA_a$ was found to be strictly arogenate and $NADP^+$ dependent. Regarding the regulation of this enzyme, some authors have found it sensitive to tyrosine feedback inhibition (Bonner et al., 2004), whereas others have not (Legrand et al., 2006). In *E. coli* the synthesis of tyrosine occurs via HPP (4-hydroxyphenylpyruvate) through the activity of the bifunctional TyrA enzyme which isomerizes chorismate to prephanate and subsequently dehydrogenates and decarboxylates 4-hydroxyphenylpyruvate (HPP). TyrA enzymatic activity over prephanate is inhibited by tyrosine (Gething et al., 1976) and feedback-resistant mutant versions of this enzyme have been generated by mutagenesis (Lütke-Eversloh and Stephanopoulos, 2005) allowing generating tyrosine overproducing *E. coli* strains.

Phenylpropanoids are a diverse group of aromatic chemicals derived from phenylalanine and tyrosine, which are produced by plants for protection against pathogens, ultraviolet irradiation and herbivores. Some phenylpropanoids are of biotechnological interest because of their use as precursors of drugs, flavors and fragrances used in the pharma, food and cosmetic industries. Notable examples include flavonoids and anthocyanins. The complex structures of industrially relevant phenylpropanoids typically make chemical synthesis impractical (Chemler et al., 2008). Extraction from the native plant sources is not economically viable because they accumulate in low quantities and they are difficult to separate from the multitude of other plant compounds with similar structures (Wu et al., 2008; Hussain et al., 2012). Several phenylpropanoids have been produced through metabolic engineering in different microorganisms. However, many phenylpropanoid biosynthetic enzymes depend upon NADPH as co-factor. Compared to photosynthetic organisms, heterotrophic ones have lower NADPH levels and the requirement for NADPH has been identified as the principal limitation for high-yield production of phenylpropanoids such as catechins in *E. coli* (Chemler et al., 2010). In this context, cyanobacteria offer a window of opportunity for heterologous production of phenylpropanoids as they possess a large pool of NADPH, produced through the photosynthetic light reactions.

All phenylpropanoids derive from *p*-coumaric acid, cinnamic acid and caffeic acid. In their own right, these acids have attractive features that make them highly valuable. For example cinnamic acid aldehyde has well documented growth inhibitory proprieties over several bacteria and yeast species (Chang et al., 2001; Guzman et al., 2014) and has proven highly effective to kill mosquito larvae (Cheng et al., 2004). *p*-Coumaric acid is valuable because it can be used as precursor for the synthesis of environmentally degradable thermoplastics (Kaneko et al., 2006). It has also been found to have antiproliferative effect on colon cancer cells (Jaganathan et al., 2013), anxiolytic effect (Scheepens et al., 2014) and nephroprotective and neuroprotective effect in rats (Navaneethan et al., 2014; Sakamula et al., 2018). Caffeic acid has been shown to have anti-inflamatory effect in rats (Chao et al., 2010) and caffeic acid phenethyl ester was shown to suppress the proliferation of human prostate cancer cells (Chuu et al., 2012).

In this work we explore the production of phenylalanine and tyrosine and their derived phenylpropanoids: cinnamic acid, *p*-coumaric acid and caffeic acid. We manipulated the genome of *Synechocystis* by introducing the feedback-inhbition-resistant enzymes $AroG^{fbr}$ in combination with $TyrA^{fbr}$ from *E. coli* in the *psbAII* locus. Additionally, we attempted to manipulate the supply of PEP and E4P precursors in two distinct ways: by overexpressing the PEP synthase enzyme (PpsA) from *E. coli* or the sigma factor SigE from *Synechocystis*. SigE is a Group 2 sigma factor known to activate the transcription of several sugar catabolic genes (Osanai et al., 2005). To convert phenylalanine and tyrosine

to phenylpropanoids we expressed XAL, an ammonia-lyase from the *Trichosporon cutaneum* yeast, which has both, phenylalanine ammonia-lyase (PAL) and tyrosine ammonia-lyase (TAL) activity (Vannelli et al., 2007). To produce caffeic acid from *p*-coumaric acid, we tested the activity of the HpaBC complex from *E. coli*. HpaBC is *E. coli* native 4-hydroxyphenylacetate 3-hydroxylase complex which has been shown capable of hydroxylating *p*-coumaric acid at the C_3 position of the phenolic ring forming caffeic acid (Lin et al., 2012b).

2. Materials and Methods

2.1. Constructs design and cloning

Genetic fragments were ordered and synthesized by Eurofins Genomics (Germany) when stated. All primers are listed in supplementary material. All reagents were supplied by New England Biolabs.

To overproduce aromatic amino acids a series of pARO integrative plasmids were built to recombine with the *psbAII* locus. Each pARO plasmid targeted a different genetic construct to the genome of *Synechocystis*. pARO-0 targeted the control construct, whereas pARO1-3 targeted each of the following genetic constructs: AT, ATS and ATP (for a detailed view of the genetic constructs see Fig. 2 and for a detailed view of the plasmids see Fig. S6). The pARO-0 vector was generated by assembly of the following fragments: pJ344 backbone (Englund et al., 2015) amplified with primers pJ-F and pJ-R; the upstream and downstream regions of *psbAII*, amplified from genomic DNA of *Synechocystis* with primers psbA2-up F plus R, and psbA2-dw F plus R, respectively.Note that the upstream fragment includes the native *psbAII* promoter. The multi cloning site and terminator sequences were amplified as one fragment from the pFERM vector (Englund et al., 2015) with primers termF and R to allow for assembly; the spectinomycin resistant gene was amplified from the pDFtrc vector (Guerrero et al., 2012) with primers specF and R. All fragments were assembled using Gibson assembly according to the manufacturer recommendations. To build pARO-1, the feedback-inhibition-resistant mutant gene versions of AroG (*aroG^{fbr}*) and TyrA (*tyrA^{fbr}*) from *E. coli* were codon optimized for cyanobacteria and synthesized as one operon fragment with genes separated by a RBS sequence. Next, the aroG^{fbr}-tyrA^{fbr} operon was amplified with primers aroG-F and tyrA-R to allow for Gibson cloning in the pARO-0 vector previously cut with SpeI-HF and de-phosphorilated with CIP (New England Biolabs). For pARO-2 construction, we ordered a codon modified version of *Synechocystis sigE* gene designed to prevent potential cross-recombination with the native gene. The gene was then amplified with primers sigE-F and sigE-R and cloned in the SpeI linearized pARO-1 vector by Gibson assembly. To build pARO-3, we ordered a codon optimized version of *E.coli's ppsA* gene. The *ppsA* gene was later amplified with ppsA-F and R to allow for Gibson cloning in the the SpeI linearized pARO-1 vector.

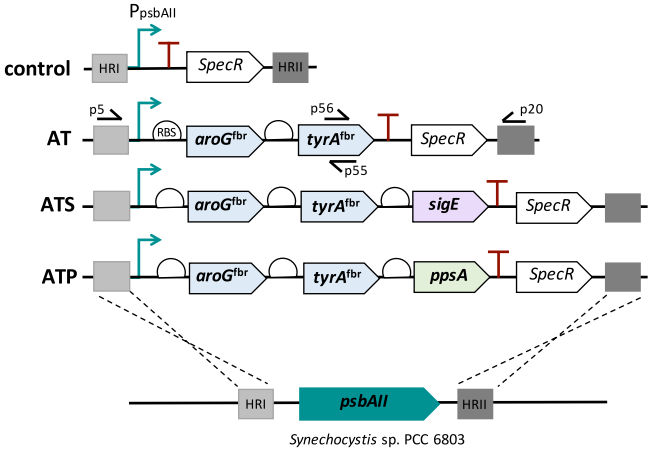

Fig. 2. Schematic representation of the genetic constructs used in this work to achieve AAA overproduction in *Synechocystis*. All constructs were designed to integrate in the genome of *Synechocystis* by homologous recombination with the upstream (HRI) and downstream (HRII) regions of the *psbAII* locus. Control construct contains no genes other than the spectinomycin resistant cassette. AT, ATS and ATP constructs were designed as operons in which the genes of interest were separated by ribosome binding sequences (RBS: AGGAGG) and driven by the *psbAII* promoter (PpsbAII). Genes from *E. coli*: *aroG^{fbr}* feedback-inhibition-resistant DAHPS; *tyrA^{fbr}* feedback-inhibition-resistant chorismate mutase/prephanate dehydrogenase; *ppsA* PEP synthase. Genes from *Synechocystis*: *sigE* group 2 sigma factor SigE.

To target the PheA enzyme to degradation, we build the integrative pPheA:Dt plasmid via Gibson assembly of four genetic fragments: the pJ334 backbone (amplified with primers lbo119 and lbo120); the slr1662:ssrA sequence (amplified from *Synechocystis* genomic DNA with primers lbo113 and lbo114 - the overhang of lbo114 also encodes the ssrA degradation tag AANDENYALAA); the nourseothricin resistance gene (amplified from an in-house vector with primers lbo115 and lbo116); and the downstream region to the *slr1662* locus (amplified from *Synechocystis* genomic DNA with primers lbo117 and lbo118). Gibson assembly of the four fragments was done according to NEB recommendations.

The aromatic amino acid overproducer (AAAOP) strains were made in a Δ*slr1573* background in order to avoid degradation of phenylpropanoids (Xue et al., 2014). The *slr1573* open reading frame encoding the laccase responsible for degradation of hydroxycinnamic acids was knocked out by inserting the kanamycin resistant gene by homologous recombination with the integrative pΔslr1573 plasmid. The plasmid was built by cloning the kanamycin resistant gene between the upstream and downstream regions of *slr1573* gene. Briefly, *Synechocystis* genomic DNA was used to amplify the upstream and downstream region of *slr1573* with primers upF and upR, or dwF and dwR respectively. Next, the *slr1573* upstream and downstream fragments, together with the kanamycin resistant gene (amplified from pFERM1 (Englund et al., 2015) with kanF and R) were assembled into the pJ344 backbone by Gibson assembly (Gibson et al., 2009).

The genes encoding the phenylpropanoids biosynthetic enzymes (accession numbers: KR095287 for XAL, and AFH14220.1 plus ADT77975.1 for the HpaBC complex) were codon optimized for Synechocystis *Synechocystis* and synthesized by Eurofins Genomics. All the coding sequences were placed in the self-replicating pDFtrc plasmid (Guerrero et al., 2012) modified for chloramphenicol resistance. First the original spectinomycin resistance cassette of pDFtrc was replaced by the chloramphenicol resistance gene. To achieve this, the spectinomycin resistant gene was removed from the vector by digestion with BsrGI and SacI. Next, the chloramphenicol resistance gene was amplified with primers CamF and CamR from an in-house vector and cloned in the resistance-less pDFtrc by Gibson assembly. To construct pDFtrcX, the codon optimized *xal* gene from *Trichosporon cutaneum* was amplified with primers awo243 and awo244. Next, pDFtrc and amplified TcXAL fragment were digested with EcoRI-HF and HindIII-HF and then ligated using T4 ligase. To build pDFtrcXH, the codon optimized *hpaBC* operon sequence from *E. coli* was amplified with primers lbo146 and lbo147 and Gibson assembled in pDFtrcX previously digested with HindIII restriction enzyme and dephosphorilated with CIP. All plasmids constructed in this work were verified by sequencing analysis (Macrogen Europe, Amsterdam).

2.2. Transformation of cyanobacteria

The integrative plasmids pΔslr1573, pAROs and pPheA:Dt were independently transformed by natural transformation. Briefly, 10 ml of WT *Synechocystis* (OD_{730} ~ 1) were spun down at 4500 × *g* for 10 min. The pellet was resuspended in 10 ml of fresh BGH11 (see below for medium details). 200 µL of cells were aliquoted and 5 µg of pΔslr1573 plasmid were added and mixed by pipetting. The cells were incubated for 4 h under 100 µE at 30 °C. Next, cells were plated in BGH5 agar

plates without antibiotics and incubated for 48 h at 30 °C and approximately 30 μE continuous illumination. Subsequently, cells were moved to BGH5 agar plates with 10 μg/ml kanamycin. Every 3 weeks colonies were re-streaked onto BGH5 plates with double the amount of kanamycin until reaching full segregation. Strains were maintained at a final kanamycin concentration of 50 μg/ml.

The integrative pARO series was likewise transformed in the Δslr1573 background but it required 10 μg of each pARO plasmid for successful transformation. Additionally, cells had to be recovered in BGH5 agar plates at 25 °C and approximately 10 μE continuous illumination under increasing concentrations of spectinomycin (starting at 5 ug/ml) to achieve full segregation (50 μg/ml). The resulting strains, collectively termed AAAOP (aromatic amino acid over-producers) were always grown in medium supplemented with 50 μg/ml kanamycin and 50 μg/ml of spectinomycin.

The pPheA:Dt plasmid was transformed in the AAAOP background by natural transformation as described above. Transformants were selected on BGH5 agar plates supplemented with 20 μg/ml nourseothricin. Positive transformants were confirmed by colony PCR with primers p168 and p169. Strains were routinely grown in medium supplemented with 50μg/ml kanamycin, 50μg/ml spectinomycin and 20μg/ml nourseothricin.

The self-replicative pDFtrcX, pDFtrcXH, or empty pDFtrc plasmids were independently transformed by triparental mating as described by Huang et al. (2010) in the phenylalanine/tyrosine overproducer AT-3 background strain and in C (control) strain. Positive transformants were selected in 50 μg/ml of kanamycin, 50 μg/ml of spectinomycin and 35 μg/ml of chloramphenicol.

2.3. Genotyping of AAAOP strains

The genotype of the AAAOP strains was confirmed by colony PCR. The control strain (resulting from pARO-0 transformation) was genotyped with with primers p5 and p20. Strains AT, ATS and ATP were genotyped using the primer combination p5 and p56 or p55 and p20 in two independent PCR reactions (see Fig. 2 for primer location). Be aware that each independent PCR reaction were loaded in the same well as shown in Supplementary Fig. S1A (in that way there should be two different bands in the same lane as each of them is the amplicon of a different primer pair). All AAAOP strains were checked for the presence of the WT *psbAII* locus with primers p5 and p20 (Supplementary Fig. S1B).

2.4. Strains and cultivation conditions

E. coli strains (NEB 10-beta) carrying pΔslr1573, pARO, pPheA:D or the different pDFtrc plasmids were grown in LB media supplemented with either 50 μg/ml kanamycin, 50μg/ml spectinomycin, 20μg/ml nourseothricin or 35μg/ml chloramphenicol respectively. HB101 *E. coli* strain, carrying the pRL443 helper plasmid, was grown in 100 μg/ml of ampicillin.

2.5. Photoautotrophic growth conditions

Cyanobacteria strains were grown on BG5 medium (Stanier et al., 1971) agar plates supplemented with 1.5 g/L HEPES (from now on called BGH5). Cultures were kept at 30 °C and approximately 30 μE continuous illuminations. Liquid cyanobacteria cultures were grown in BG11 media (Stanier et al., 1971) supplemented with 4.75 g/L HEPES (from now on called BGH11) with constant supply of air enriched with 3% (v/v) CO_2 at 30 °C and approximately 50 μE of continuous light. Whether in plates or liquid, cyanobacterial strains were always supplemented with appropriated antibiotics (see above for details on each specific strain).

For analysis of metabolite production under photoautotrophic conditions strains were grown in BGH11. Firstly, 20 ml liquid pre-cultures were inoculated from plate-grown cultures, and grown in an aquarium tank as described above for 3 days. Then, cultures were spun down and washed twice with fresh medium before re-inoculation to an OD_{730} ~ 0.2 in 80 ml culture vessels and grown in a Multi-Cultivator MC 1000-OD (Photon Systems Instruments) with 1 mM IPTG, appropriated antibiotics and constant supply of 3% (v/v) CO_2 and 100 μE continuous illumination for the specified number of days. Samples for LC-MS were collected upon inoculation and after the specified number of days as indicated in each figure for LC-MS analysis as described below.

Strains with PheA enzyme targeted for degradation were grown on BGH11 medium with constant supply of air enriched with 3% (v/v) CO_2 at 30 °C and approximately 50 μE of continuous light. Samples were taken after 48 h of photoautotrophic growth and prepared for LC-MS analysis as described below.

2.6. Dry weight determination

The control strain was grown in a Multi-Cultivator MC 1000-OD (Photon Systems Instruments) at 100 μE continuous illumination for nearly 6 days in BGH11 medium. Every day, four 20 ml samples were harvested and the optical density at 730 nm was measured in a Ultraspec 3100 Pro UV/Visible Spectrophotometer (GE Healthcare/Amersham Biosciences). Next, each sample was filtered through a 0.45 μm hydrophilic PVDF filter (Durapore Membrane Filter, Sigma-Aldrich), which had previously been dried for 24 h at 70 °C in a Shel-lab oven (Sheldon Manufacutring Inc). The filtered biomass was washed twice with 20 ml Milli-Q water and dried for 24 h at 70 °C. Dry filters coated with biomass where then allowed to cool down in a desiccator and subsequently weighted in a MTxs204 delta range balance (Mettler Toledo). Biomass values for OD ranging from 0 to 5 were thereby experimentally determined. The measured milligrams of biomass per liter of culture were plotted against their respective OD values showing a linear relationship. Linear regression reveals a slope of 0.19497 ($R^2 = 0.98$). This relation was used for all of the strains in this work because their biomass data appeared to be well described by the fit (green and blue dots in Supplementary Fig. S3).

2.7. Glycogen determination

Glycogen determination was done as described by Osanai et al., 2011. Briefly, ~ 6 x 10^8 cells were subjected to acidic hydrolysis by resuspension in 100 μL of 3.5% (v/v) sulfuric acid and 40 min of boiling. Samples where then centrifuged for 1 min and the supernatant was mixed with 350 μL of 10% Trichloroacetic acid followed by 5 min incubation at room temperature. For the blank 100 μL of water where used instead. Samples and blank were then centrifuged for 5 min; subsequently 150 μL of supernatant were mixed with 750 μL of 6% *o*-toluidine (diluted in glacial acetic acid). Next, samples and blank were boiled for 10 min followed by 3 min cooling a room temperature in a water bath. Lastly, the amount of glycogen was monitored by the absorbance at 635 nm. To allow for glycogen quantification a glucose standard curve with concentrations ranging from 0 to 1 mg/mL was performed. The linear regression reveled a slope of 0.5247 ($R^2 = 0.99$).

2.8. Sample preparation and LC-MS analysis

For analysis of AAA and phenylpropanoids production, total cultures (including cells and medium) where harvested upon inoculation and after the number of days indicated in each figure. Samples were extracted by mixing them with an equal volume of 40% methanol. Samples were subsequently diluted 5 times more with 20% methanol prior to storage at −20 °C until analysis. For amino acids determination, samples were diluted 10 times further to final 2% (v/v) methanol concentration using a mix of ^{13}C-, ^{15}N-labeled amino acids at known concentrations. To quantify chemical content inside of the cells, 1 mL of culture was harvested and pelleted by centrifugation at 4000 × *g* and

the supernatant was removed. Pellets were extracted by resuspension in 500 µL of 40% methanol. Next, samples were topped up with 500 µL of 20% methanol. Prior to LC-MS analysis samples were diluted 10 times with a mix of ^{13}C-, ^{15}N-labeled amino acids at known concentrations. All samples were filtered through a 2 µm filter prior to LC-MS injection.

Quantification of metabolites was carried out by liquid chromatography mass spectrometry (LC-MS) on a Bruker EVOQ Elite triple quadrupole MS as previously described (Mirza et al., 2016). Briefly, chromatographic separation was achieved on a Zorbax Eclipse XDB-C18 column (3.0 × 100 mm, 1.8 µm, Agilent Technologies) with a flow rate of 500 µl/min and column temperature set to 40 °C). The following gradient with 0:05% formic acid in water (v/v) as solvent A and acetonitrile (+0:05% formic acid (v/v)) as solvent B was used: 0.0–1:2 min 3% B; 1.2–3:8 min 3–65% B; 3.8–4 min 65–100% B; 4.0–4:6 min 100% B; 4.6–4:7 min 100-3% B and 4.7–6 min 3% B. Ionization was carried out in positive and negative ionization mode with spray voltage at 4000V and −3000 V, respectively. Probe temperature was maintained at 300 °C and probe gas flow set to 50 psi. Nebulizing gas was set to 60 psi and collision gas to 1.6 mTorr. Nitrogen was used as probe and nebulizing gas and argon as collision gas. Active exhaust was constantly on. Individual metabolites were detected by multiple reaction monitoring (MRM). MRM transitions for amino acids were chosen as previously described (Mirza et al., 2016) and for phenylpropanoids as detailed in Supplementary Table S2. Amino acids were quantified by comparison to the labeled amino acid standards while phenylpropanoids were quantified through standard curves for each individual analyte. Standard curves for each metabolite were constructed using a dilution series of pure reference compounds ranging from 2000 to 3.9 pg/µl. All chemicals were purchased from Sigma-Aldrich except for ferulic acid glucoside which was in-house synthesized and the 13C-, 15N-labeled amino acids (Algal amino acids 13C, 15N, Isotec, Miamisburg, US).

3. Results

3.1. Engineered strains

To investigate whether it was possible to overproduce AAA, particularly phenylalanine and tyrosine in *Synechocystis*, we designed three different genetic constructs (AT, ATS, ATP) (Fig. 2) to individually integrate in the genome of *Synechocystis*. The AT construct carries the *aroG^{fbr}* and *tyrA^{fbr}* genes, which encode feedback-inhibition-resistant mutant versions of the enzymes AroG (DAHP synthase) and TyrA (chorismate mutase/prephenate dehydrogenase) from *E. coli*. With this we aimed at redirecting the carbon flow from the central metabolism into the Shikimate and the phenylalanine/tyrosine biosynthetic pathways. In addition to *aroG^{fbr}* and *tyrA^{fbr}*, the ATS construct bears the *sigE* gene. Thereby we aimed at enhancing the supply of AAA precursors: PEP and E4P which derive from the central carbon catabolism. Besides *aroG^{fbr}* and *tyrA^{fbr}* the ATP construct contains the *ppsA* gene, which encodes a *E. coli* PEP synthase to increase PEP supply. In every construct, genes were organized as an operon driven by the strong, light-inducible *psbAII* promoter. Operons were located in between the upstream and downstream regions of the endogenous *psbAII* locus and thus integrated in the cyanobacterial genome by homologous recombination with each respective carrier plasmid as explained in Material and Methods. The resulting strains were named after the integrated construct and we collectively refer them as AAAOP (aromatic amino acid overproducer) strains (Fig. 2). The control construct and resulting strain only contain the spectinomycin resistance gene.

We isolated three biological replicates for each AAAOP genotype and genotyped them as described in Materials and Methods. All strains show the expected amplicon band sizes for the inserted constructs and full segregation except colony ATP-3 which showed presence of the WT psbAII gene (Supplementary Figure S1 A).

Table 1
Average production of aromatic amino acids for each strain of each genotype after 72 h of autotrophic growth (constant 3% (v/v) CO2 supply and 100 µE light) as measured by LC-MS. The colored box indicate the best producers of their genotype which were chosen for further analysis. Standard deviation values for three technical replicates.

Strain	Phe (mg/l)	Tyr (mg/l)	Trp (mg/l)
Control 1	0.70 ± 0.03	0.25 ± 0.39	0.11 ± 0.16
AT-1	43.65 ± 6.14	2.09 ± 0.96	1.31 ± 0.07
AT-2	0.91 ± 0.08	0.14 ± 0.05	0.02 ± 0.002
AT-3	63.71 ± 3.07	2.75 ± 1.21	1.84 ± 0.04
ATS-1	60.47 ± 4.13	2.47 ± 0.17	1.40 ± 0.02
ATS-2	66.55 ± 1.89	3.92 ± 1.84	1.57 ± 0.13
ATS-3	43.90 ± 1.38	1.37 ± 0.04	0.97 ± 0.02
ATP-1	41.76 ± 1.82	3.97 ± 1.70	1.71 ± 0.07
ATP-2	47.62 ± 2.56	2.59 ± 0.39	1.87 ± 0.06
ATP-3	53.84 ± 4.90	3.51 ± 0.63	2.03 ± 0.04

3.2. Overproduction of phenylalanine and tyrosine in Synechocystis is possible

To test whether the production of AAA in the AAAOP strains was affected compared to the control strain we grew them under photoautotrophic conditions for 72 h as described in Materials and Methods. The concentration of AAA was measured by LC-MS. Table 1 lists how many milligrams per liter of each AAA were produced by each biological replicate of each genotype, as well as for the control. Strains AT-3 and ATS-2 showed the highest production of phenylalanine and tyrosine amongst their genotypes therefore we subjected them to further analysis. Among the ATP colonies we selected ATP-2 for further analysis because, although ATP-3 showed the highest production of its genotype it did not show full segregation for the *psbAII* locus (Supplementary Figure S1 B).

To assay the full production potential of AT-3, ATS-2 and ATP-2 under photoautotrophic conditions we grew each strain as indicated above for 10 days. Fig. 3 shows the representative time course production of AAA in the control, AT-3, ATS-2 and ATP-2 strains during 10 days of photoautotrophic growth. Strain AT-3 consistently showed to be the best producing strain reaching a maximum production of 579.8 ± 33.8 mg/L of phenylalanine and 41.1 ± 2.3 mg/L of tyrosine after 10 days of photoautotrophic growth. AT-3 also showed the highest production of tryptophan: 12.4 ± 1.8 mg/L. Phenylalanine production after 10 days in strains ATS-2 and ATP-2 was 391.8 ± 26.5 and 322.6 ± 13.1 mg/L respectively. Whereas tyrosine production reached 35.6 ± 2.6 mg/L in ATS-2 and 25.1 ± 2.1 mg/L in ATP-2. Tryptophan was also higher in those two strains than in control: 6.4 ± 1.6 or 7.7 ± 1.5 mg/L versus 0.06 ± 0.01 mg/L in the control strain. The levels of phenylalanine and tyrosine in the control strain after 10 days of photoautotrophic growth were 0.22 ± 0.03 and 0.10 ± 0.04 mg/L respectively. Interestingly, on average less than 1% of all phenylalanine was present in the cell fraction of either genotype with more than 99% of phenylalanine present in the medium. In the case of tyrosine, around 90% on average was recovered from the medium versus 10% present in the cell pellets of either phenotype (Supplementary Fig. S2).

To compare strains, the AAA production was normalized to biomass content. To achieve this, we determined the relationship between optical density at 730 nm and grams per liter of biomass for the control strain (Supplementary Fig. S3). The relationship was linear with a measured slope of 0.19497 ± 0.005 (R^2 = 0.98). This relation was also used for the AAAOP strains because their biomass data appeared to be well described by the fit (green and blue dots in Fig. S3). Fig. 4 A-C shows the normalized production of phenylalanine, tyrosine and tryptophan in the AAAOP strains and control after 10 days of photoautotrophic growth. Consistently through experiments, the AT-3 strain showed the highest production: 903.8 ± 52.7 mg/gDW of phenylalanine, 64.04 ± 3.67 mg/gDW of tyrosine and 19.3 ± 2.8 mg/gDW of tryptophan.

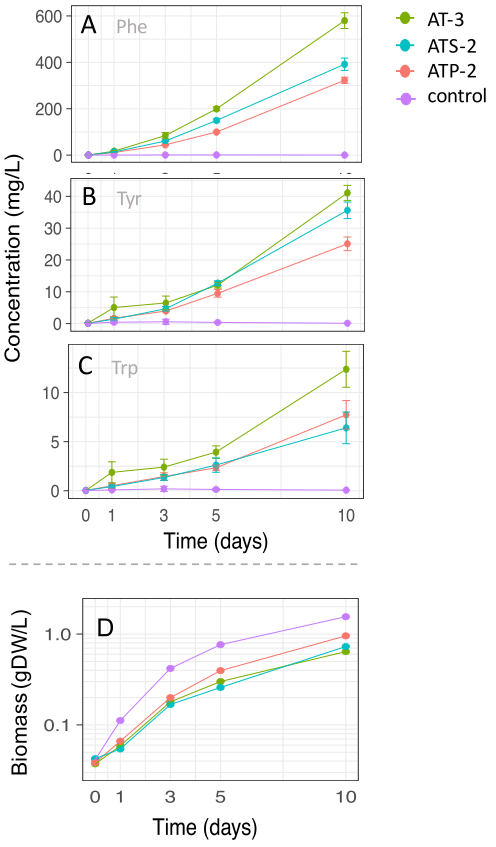

Fig. 3. Time course of AAA concentration and biomass production for each AAAOP strain and control. Control strain in purple; AT-3, ATS-2 and ATP-2 strains in green, blue and red respectively. Time indicates days of photoautrophic growth in BGH11 medium. (A) Phenylalanine production. (B) Tyrosine production. (C) Tryptophan production. (D) Growth plotted as dry biomass density over time (10 days) for AAAOP strains and control grown in BGH11 medium. Notice the logarithmic scale. Error bars are standard deviation values for three technical replicates. All stains were grown under the same antibiotic pressure. . (For interpretation of the references to color in this figure legend, the reader is referred to the Web version of this article.)

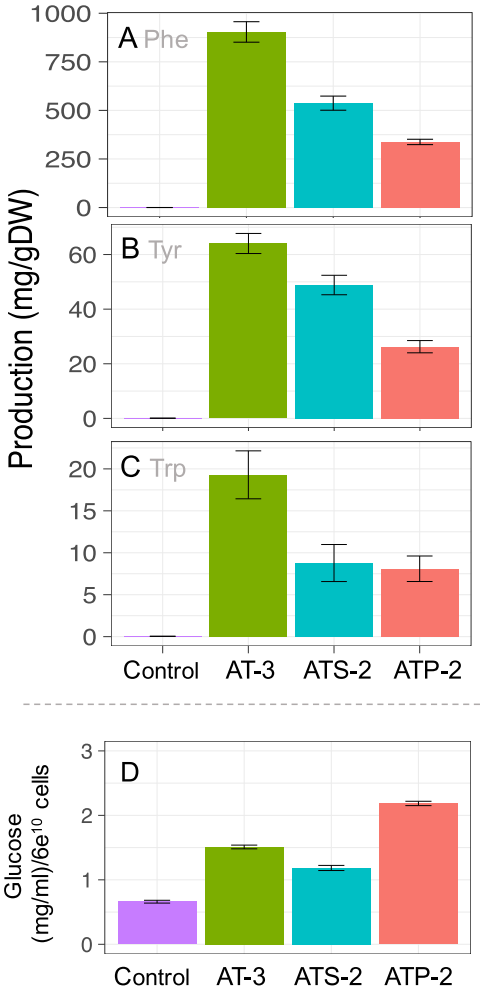

Fig. 4. Normalized production of AAA and glycogen content for each AAAOP strain and control. Control strain in purple; AT, ATS and ATP strains in green, blue and red respectively. (A) Phenylalanine. (B) Tyrosine. (C) Tryptophan. (D) Glycogen measured as mg/ml of glucose in ~ 6 x 10^8 cells of each strain grown for 72 h in 3% (v/v) CO_2 and continuous 100 uE of light. Error bars represent standard deviation values of three technical replicates. . (For interpretation of the references to color in this figure legend, the reader is referred to the Web version of this article.)

Regarding growth, all three AAAOP strains grew less than the control strain, which reached 1.55 g/L of biomass (Fig. 3D), with the highest AAA overproducer, strain AT-3 reaching the lowest levels of biomass: 0.6 g/L. This was less than half of the biomass produced by the control after 10 days of photoautotrophic growth in BGH11 medium (constant 3% (v/v) CO_2 and 100 μE of light).

Remarkably, in the AT-3 strain, the production of the three AAA combined after 10 days reached ~987 mg/gDW which means that the weight of accumulated AAA was roughly equal to the dry weight. Without the over-production burden, the control strain invested all its carbon in growth, producing roughly double the biomass than the AT-3 strain. The ATS-2 and ATP-2 strains are consistent with this overall behavior showing a negative correlation between growth and AAA production.

3.3. AAA overproduction affects glycogen accumulation

We expected that increased production of aromatic amino acids in general and that in particular the attempted overexpression of sigE would affect the amount of carbon stored in glycogen. To test this we sampled ~6 x 10^8 cells after 72 h of photoautotrophic growth and determined glucose levels as described in Material and Methods. During photoautotrophic growth conditions under continuous light (Fig. 4D) all three AAAOP strains showed to accumulate significantly more glycogen than the control strain. ATP-2 showed the highest accumulation of glycogen, followed by AT-3 and ATS-2.

3.4. Degradation of PheA (predicted prephanate dehydratase) results in lower phenylalanine and tyrosine production

In *E. coli* it was possible to increase tyrosine production by knocking out the bifunctional chorismate mutase/prephanate dehydratase PheA from a phenylalanine overproducer strain (Olsonet al., 2007). In *Synechocystis* the *sll1662* locus has been predicted to encode PheA with prephanate dehydratase activity and potentially also arogenate dehydratase activity (Fig. 1). Knocking out this gene from the AAAOP strains could potentially increase the tyrosine levels since more prephanate and arogenate would be available for tyrosine biosynthesis. To test this hypothesis we decided to target the *sll1662* gene with the ssrA degradation tag by homologous recombination of the pPheA-Dt plasmid with the AT-3 strain (Fig. 5).

The resulting strains, named AT-3-Dt, showed full segregation for the PheA-Dt construct in *sll1662* locus (Supplementary Fig. S4) and were capable to grow without phenylalanine supplementation. To test how the production of tyrosine and phenylalanine was affected in the

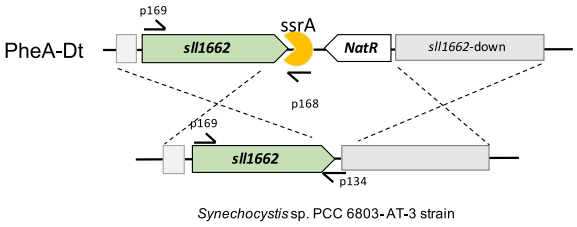

Fig. 5. Schematic representation of the PheA-Dt construct designed to recombine with the *sll1662* locus from the AT-3 strain, and target the resulting protein: PheA (prephanate dehydratase) for degradation. ssrA represents the degradation. NatR stands for the nourseothricin resistance gene.

Table 2
Normalized production of aromatic amino acids in AT-3 and AT-Dt1-3 strains after 48 h of growth with constant supply of 3% (v/v) CO2 and 50 μE of light. Abbreviations: Phe, phenylalanine; Tyr, tyrosine.

Strain	Phe (mg/gDW)	Tyr (mg/gDW)
AT-3	57.1 ± 3.5	11.2 ± 1.2
AT-3-Dt1	1.9 ± 0.2	2.5 ± 0.1
AT-3-Dt2	1.1 ± 0.01	1.3 ± 0.02
AT-3-Dt3	4.7 ± 5.3	9.9 ± 7.6

AT-3-Dt strains compared to AT-3, we grew three biological replicates under photoautotrophic conditions with constant supply of 3% (v/v) CO_2 and 50 μE of light. The amount of each AAA was determined by LC-MS analysis after approximately 48 h of growth (three technical replicates for each biological replicate where analyzed by LC-MS). Measured values are shown in Table 2. Results showed a reduction in phenylalanine accumulation of more than 10 fold in the AT-3-Dt strains compared to the control AT-3 strain. Surprisingly, levels of tyrosine were also lower in all the AT-3-Dt strains.

3.5. Production of p-coumaric acid and cinnamic acid from tyrosine and phenylalanine

To produce *p*-coumaric acid and cinnamic acid in *Synechocystis* we cloned the gene encoding the XAL enzyme from *Trichosporon cutaneum* in the self-replicative pDFtrc vector as explained in Material and Methods. XAL has both, phenylalanine ammonia-lyase (PAL) and tyrosine ammonia-lyase (TAL) activity, it therefore produced cinnamic acid and *p*-coumaric acid from phenylalanine and tyrosine, respectively. The resulting pDFtrcX plasmid (Fig. 6B) was transformed into the phenylalanine/tyrosine overproducer AT-3 background strain. As control we transformed the pDFtrcX plasmid in a non-AAA-overproducer background strain. Note that the *slr1573* gene, known to encode a laccase responsible to degrade *p*-coumaric acid (Xue et al., 2014), had been knocked out in both background strains by the kanamycin resistance gene. The resulting strains, termed X1–3 (three biological replicates) and cX for the control, were genotyped positive for the presence of the pDFtrcX plasmid (Supplementary Fig. S5A) and subjected for analysis of cinnamic acid and *p*-coumaric acid production. An AT3-Δ*slr1573* strain carrying the empty pDFtrc plasmid was also analyzed for production of all phenylpropanoids of interest and none was found (data not shown) therefore it is disregarded in the following results.

To test whether the XAL bearing strains are capable to produce cinnamic acid and *p*-coumaric acid, we analyzed by LC-MS samples of cultures grown photoautotrophically for 5 days and normalized the results to biomass content in order to compare strain performance. The LC-MS analysis showed that both, cinnamic acid and *p*-coumaric acid were produced in all strains indicating that XAL is active (Table 3). The X3 strain showed to be the best one, producing 470.0 ± 70.6 mg/gDW of p-coumaric acid and 267.2 ± 31.8 mg/gDW of cinnamic acid after 5 days of photoautotrophic growth. This production is ~12 fold more p-coumaric acid or cinnamic acid than the cX control strain produced. The vast majority of cinnamic acid and *p*-coumaric acid was secreted to the medium and less than 1% of all *p*-coumaric acid or cinnamic acid was found in the cell pellet fraction. After five days of photoautotrophic growth, the levels of phenylalanine and tyrosine in all strains were very low: in the X3 strain we detected 6.4 ± 1.9 and 4.5 ± 2.6 mg/gDW of phenylalanine and tyrosine respectively. In the cX control strain we measured 0.2 ± 0.1 mg/gDW of phenylalanine and 0. 2 ± 0.1 mg/gDW of tyrosine. After 5 days of photoautotrophic growth, the cX strain grew the most, reaching 894 mg of dry biomass per liter of culture whereas the X3 strain reached only half of the biomass accumulated by the cX control (Table 3).

3.6. Production of caffeic acid by active HpaBC complex in Synechocystis

To produce caffeic acid from *p*-coumaric acid we introduced the pDFtrcXH plasmid in the AT-3 and Control background strains (Fig. 6C). Besides XAL, the pDFtrcXH plasmid contains the genes

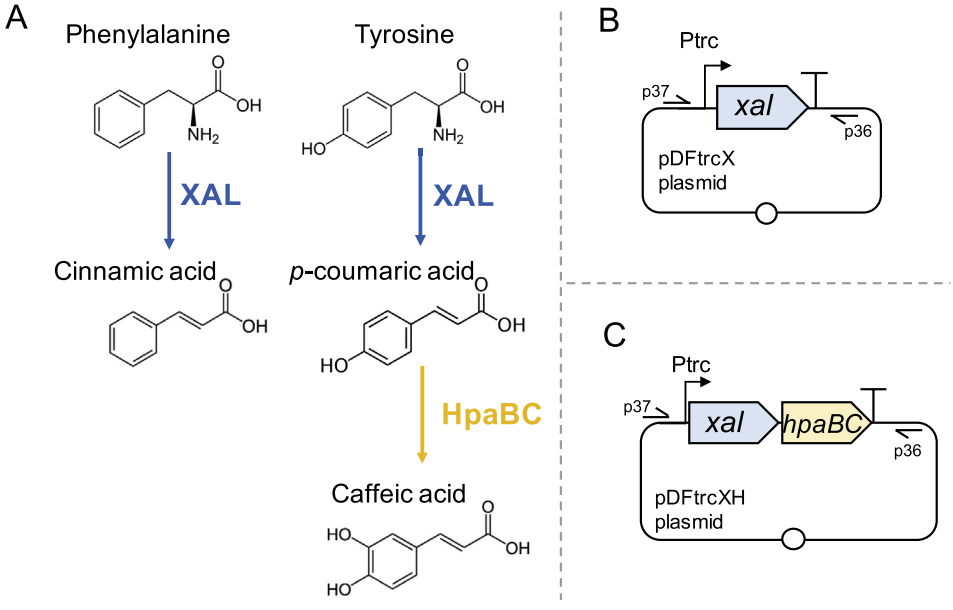

Fig. 6. Schematic representation of the biosynthetic pathway and plasmids used to produce phenylpropanoids. (A) schematic representation of phenylpropanoids biosynthetic pathway used in this work. XAL has phenylalanine ammonia-lyase activity producing cinnamic acid, as well as tyrosine ammonia-lyase activity producing *p*-coumaric acid. HpaBC hydroxylates *p*-coumaric acid at the C_3 position of the phenolic ring forming caffeic acid. (B) schematic representation of the self-replicative pDFtrcX plasmid used to express the XAL enzyme (*xal*). (C) schematic representation of the self-replicative pDFtrcXH plasmid used to express XAL and HpaBC enzymes (*xal, hpaBC*). p37 and p38 represent the primers used to genotype the plasmids.

Table 3
Concentration (mg/gDW) of phenylalanine (Phe), tyrosine (Tyr), tryptophan (Trp), *p*-coumaric acid (pCA) or cinnamic acid (CiAc) and biomass (mg/L) produced by each strain after 5 days of photoautotrophic growth.

Strain	Compound (mg/gDW)					Biomass (g/L)
	Phe	Tyr	Trp	*p*CA	CiAc	
X1	17.5 ± 11.4	20.3 ± 16.5	8.5 ± 3.5	448.3 ± 6.3	238.1 ± 37.3	0.393
X2	3.4 ± 1.2	2.7 ± 2.1	0.5 ± 0.4	156.0 ± 4.3	85.9 ± 8.63	0.627
X3	6.4 ± 1.9	4.5 ± 2.6	6.0 ± 1.4	470.0 ± 70.6	267.2 ± 31.8	0.426
cX	0.2 ± 0.1	0.2 ± 0.1	0.1 ± 0.03	42.7 ± 3.5	20.5 ± 2.2	0.894

Table 4
Concentration (mg/gDW) of phenylalanine (Phe), tyrosine (Tyr), tryptophan (Trp), *p*-coumaric acid (pCA), cinnamic acid (CiAc) or caffeic acid (CafAc) and biomass (mg/l) produced by each strain after 6 days of photoautotrophic growth.

Strain	Compound mg/gDW						Biomass (g/L)
	Phe	Tyr	Trp	*p*CA	CiAc	CafAc	
XH1	4.5 ± 2.8	4.1 ± 5.6	5.6 ± 1.3	340.2 ± 43.6	255.9 ± 72.3	34.4 ± 2.8	0.275
XH2	4.8 ± 2.1	4.5 ± 6.2	2.3 ± 0.8	161.4 ± 1.9	173.1 ± 5.6	47.4 ± 13.9	0.265
XH3	4.3 ± 0.2	0.7 ± 0.3	3.7 ± 0.3	300.0 ± 17.5	251 ± 96.7	39.9 ± 22.8	0.277
cXH	1.5 ± 2.3	2.9 ± 4.8	0.6 ± 0.9	6.2 ± 0.3	13.2 ± 3.0	4.1 ± 0.8	0.688

encoding the HpaBC complex from *E. coli*. HpaBC has been shown capable of hydroxylating *p*-coumaric acid to caffeic acid (Lin et al., 2012). The resulting strains, termed XH1–3 (three biological replicates) or cXH for the control, were genotyped positive for the presence of the pDFtrcXH plasmid (Supplementary Fig. S5B). To test the production of phenylpropanoids, all four pDFtrcXH bearing strains were grown photoautotrophically for 6 days and cultures samples were analyzed by LC-MS. Table 4 shows the production of *p*-coumaric acid, cinnamic acid, caffeic acid and aromatic amino acids normalized to biomass content after 6 days of photoautotrophic growth. The production of phenylpropanoids was an order of magnitude higher in the XH1–3 strains than in the cXH control, indicating that phenylalanine and tyrosine overproduction is needed in order to achieve high phenylpropanoid production. The XH2 strain achieved the highest production of caffeic acid: 47.4 ± 13.9 mg/gDW. After 6 days of photoautotrophic growth all XH strains showed high levels of unconverted *p*-coumaric acid. The phenylalanine and tyrosine content in the XH2 strain after 6 days was 4.8 ± 2.1 mg/gDW and 4.5 ± 6.2 mg/gDW respectively. Caffeic acid levels in the control strain only reached 4.1 ± 0.8 mg/gDW. On average only 1.5% of all caffeic acid was present in the cell pellet fractions of each culture. During this time the cXH control reached the highest biomass production (0.688 g of dry biomass per liter of culture) whereas none of the XH1–3 strains reached less than 0.3 g of dry biomass per liter of culture.

3.7. Discussion

In this study, we engineered the metabolism of *Synechocystis* to overproduce phenylalanine and tyrosine, as well as to convert those AAA into their derived phenylpropanoids: *p*-coumaric acid, cinnamic acid and caffeic acid.

The highest production of phenylalanine and tyrosine was achieved for strain AT-3 after 10 days of photoautotrophic growth (Fig. 4A–C). AT-3 was engineered to express the *aroG*^{fbr} and *tyrA*^{fbr} genes from *E. coli*. The production of 903.8 ± 52.7 mg/gDW of phenylalanine and 64.04 ± 3.67 mg/gDW of tyrosine strongly suggests successful expression of the introduced genes. For unknown reasons the clone strain AT-2 did not show overproduction of AAA (Table 1) despite the fact of test positive for a full segregated *aroG*^{fbr} *–tyrA*^{fbr} genotype (Supplementary Fig. 1).

In *E. coli*, overexpression of AroG^{fbr} and TyrA^{fbr} lead to the accumulation of 20-fold more tyrosine than phenylalanine (Lütke-Eversloh and Stephanopoulos, 2007), however in *Synechocystis* it led to the opposite situation: roughly 15 times more phenylalanine than tyrosine were produced (Fig. 4A-B). The introduced TyrA^{fbr} enzyme from *E. coli* has chorismate mutase and prephanate dehydrogenase activity, therefore it is capable of converting chorismate to prephanate and then dehydrogenate prephanate to HPP for tyrosine synthesis. Chorismate can also be used by *Synechocystis* to synthesize tryptophan. The low amount of tryptophan measured for AT-3 (Fig. 4C) suggests that TyrA^{fbr} chorismate mutase activity is high, effectively converting most of the chorismate to prephanate. Our results show that in the AT-3 strain most of the prephanate must be subsequently used to produce phenylalanine rather than used to produce tyrosine, indicating that if TyrA^{fbr} prephanate dehydrogenase activity exists in *Synechocystis*, the resulting HPP cannot be transamminated to tyrosine by the native HisC/AspC transaminases unlike predicted by homology in the KEGG.

In *Synechocystis*, tyrosine originates from arogenate by the activity of the native TyrA$_a$ enzyme whose dehydrogenase activity was found to be strictly arogenate dependent (Bonner et al., 2004; Legrand et al., 2006). Phenylalaine is thought to be synthesized via PPN through the prephanate dehydratsase activity of PheA encoded by *sll1662*. PheA is also predicted to have arogenate dehydratase activity, which means that it could potentially steal arogenate from TyrA$_a$ to produce phenylalanine. However, no experimental evidence has so far been published on *Synechocystis*'s PheA substrate specificity or regulation. The fact that in the present work we can produce phenylalanine in excess indicates that in *Synechocystis* PheA activity is not negatively regulated by phenylalanine. Interestingly, in *E. coli*, knocking out the *pheA* gene led to the conversion of a phenylalanine overproducing strain into a tyrosine overproducing strain as all prephanate got available for tyrosine synthesis (Olson et al., 2007). To test whether this could also be the case in *Synechocystis*, we used the AT-3 strain to fuse the PheA coding locus: *sll1662* to a ssrA degradation tag. When this degradation tag was added to the *yfp* gene sequence and expressed in *Synechocystis*, 95% of all YFP was targeted for degradation (Landry et al., 2013). Our results show that in the resulting strains (AT-3-Dt) phenylalanine levels were dramatically reduced compared to the AT-3 parental strain (Table 2), sustaining evidence for PheA function as the only phenylalanine biosynthetic enzyme in *Synechocystis*. With the flow towards phenylalanine reduced, more prephanate and arogenate should be available to be converted to tyrosine. However, tyrosine levels were also lower in the AT-3-Dt strains than in the parental AT-3. This could indicate that flow of prephanate towards tyrosine is tightly regulated or

that prephanate dehydrogenase activity of the introduced TyrA^{fbr} has more affinity for prephanate than the native prephanate amino transferase (PAT) responsible for arogenate synthesis. To the best of our knowledge, such PAT has never been characterized in *Synechocystis*. Another hypothetical reason that could explain the tyrosine drop in the AT-3-Dt strains could be the reliance of PAT upon phenylalanine as amino group donor for amination of prephanate into arogenate. In this hypothetical scenario, low phenylalanine levels would also result in less arogenate despite increased levels of prephanate precursor. Furthermore, albeit it has never been described, it is tempting to speculate that *Synechocystis* could have a phenylalanine hydroxylase enzyme (PheH) responsible for tyrosine production from phenylalanine, whose activity would be diminished in the PheA:ssrA background leading to the observed low tyrosine levels. PheH catalyzes the hydroxylation of phenylalanine into tyrosine and besides animals, it has been found in several bacteria species such as *Pseudomonas putida*, as well as in the chloroplasts of *Pinus taeda*, *Physcomitrella patens*, and *Chlamydomonas reinhardtii* (Zhao et al., 1994; Pribat et al., 2010).

Several studies in *E. coli* showed a significant increase in the production of phenylalanine or tyrosine by enhancing the availability of the two precursor substrates PEP and E4P (Patnaik et al., 1995; Báez-Viveros et al., 2004; Lütke-Eversloh and Stephanopoulos, 2007; Juminaga et al., 2012). To test whether this could also be the case for cyanobacteria, we combined the PEP synthase gene (*ppsA*) or the sigma factor E gene (*sigE*) with AroG^{fbr} and TyrA^{fbr}. Surprisingly, the ATS-2 and ATP-2 strains produced less AAA than AT-3 (Fig. 4B–D). The marked increase of glycogen in the ATP-2 strain (Fig. 4 D) strongly suggests that PpsA is actively converting pyruvate to PEP, thereby possibly rerouting carbon away from the tricarboxylic acid cycle, towards glycogen formation. Osanai et al. (2011) showed that overexpression of SigE (driven by PpsbAII) in *Synechocystis* led to increased transcription of genes for the oxidative pentose phosphate pathway (OPPP) and the SigE overexpressor accumulated less glycogen. We hypothesized that SigE overexpression could lead to increased flow of carbon towards E4P and more PEP available for DAHP synthesis. The accumulation of less glycogen in ATS-2 than in AT-3 under continuous light (Fig. 4 D) suggests that SigE is indeed expressed and functional in the ATS-2 strain. Although, it would be necessary to confirm that glycogen catabolic enzymes are increased in ATS-2, the carbon mobilized from glycogen is not used to synthesize more AAA. Metabolomics and proteomics experiments would shed light on the subjacent cause for decreased AAA production in the ATS-2 and ATP-2 strains.

Interestingly, AAA overproduction induced glycogen accumulation (Fig. 4 D), although the amount accumulated depended on the genotype. Thus, the ATS-2 strain, overexpressing SigE (known to activate glycogen catabolism) showed lower glycogen levels than AT-3, whereas ATP-2 accumulated more glycogen than AT-3, presumably due to carbon rerouting towards gluconeogenesis (see above for detailed discussion). It is unclear how AAA overproduction induces glycogen accumulation. Nitrogen starvation is known to trigger glycogen accumulation therefore one hypothesis could be that the AAAOP strains are nitrogen starved. All nitrogen used by the AAAOP strains to grow and overproduce AAA is provided in the form of 1.5 g/L of sodium nitrate at the beginning of each experiment. Of that sodium nitrate 16% is molecular nitrogen, corresponding to 240 mg/L. Table 5 shows how much nitrogen is present in the biomass and in each AAA produced by the AT-3 strain after 10 days of growth in BGH11. The combination of the three AAA produced contained a total of 53.96 mg/L of molecular nitrogen. Shastri and Morgan, (2005) reported that *Synechocystis* biomass is constituted of 11.29% nitrogen, hence the AT-3 strain contained 67.74 mg/L of molecular nitrogen in the 600 mg of biomass it produced after 10 days of growth. The sum of nitrogen in biomass and produced AAA corresponded to approximately 51% of the initially provided amount. Thus, we conclude that shortage of nitrogen cannot cause nitrogen starvation in the AAAOP strains grown in BGH11. Although, the shortage of extracellular nitrogen is apparently not the cause of nitrogen starvation, a possible shortage of metabolic nitrogen cannot be ruled out. The nitrogen starvation signal is triggered by high levels of 2-oxoglutarate (2OG). AspC and HisC, the two predicted aminotransferases responsible to aminate phenylpyruvate (PPN) to phenylalanine have been proposed to use glutamate as amine group donor. The deamination of glutamate results in 2OG. It can be hypothesized that the production of the high levels of phenylalanine reported for the AT-3 strain, could lead to increased production of 2OG, which in turn could trigger the nitrogen starvation signal. Hence measuring the levels of 2OG would be necessary to shed light on this matter.

Table 5
Nitrogen (N) content in the biomass and in each AAA produced by AT-3 after 10 days of photoautotrophic growth in BGH11.

	Total (mg/L)	N content (%)	N content (mg/L)
Phe	579.7 ± 33.8	8.47	49.1 ± 2.8
Tyr	41.1 ± 2.3	7.7	3.16 ± 0.17
Trp	12.4 ± 1.8	13.7	1.7 ± 0.25
Biomass	600	11.29	67.74
			Σ 121.7 ± 3.22

Overall, the best production of AAA was achieved by the AT-3 strain grown for 10 days under photoautotrophic growth conditions. It is interesting to determine how much of the fixed carbon was devoted for AAA production by this strain. Young et al. (2011) showed that each gram of dry *Synechocystis* biomass contains 41 mmol of carbon, this means that 49% of *Synechocystis* dry biomass is molecular carbon. Shastri and Morgan, (2005) reported a similar value. Based on this, we estimate that after 10 days of photoautotrophic growth the control strain contained 763.58 mg/L of molecular carbon in the 1552 mg/L of dry biomass it produced. Fig. 3 shows that the amounts of AAA produced by the control strain are negligible, therefore, assuming that no carbon is lost for respiration, 763 mg/L is the estimated carbon fixed by the control strain in 10 days of photoautotrophic growth. In the same time under the same conditions, the AT-3 strain produced 641 mg/L of dry biomass, containing 315 mg/L of carbon. However, during this time, the AT-3 strain also produced a total of 579.7 mg/L of phenylalanine, 41.08 mg/L of tyrosine and 12.3 mg/L of tryptophan (Fig. 3). As is shown in Table 6 the percentage of carbon content in these three AAA is 65% (Phe), 60% (Tyr) and 65% (Trp). Therefore, the carbon contained in each AAA produced by the AT-3 strain after 10 days of photoautotrophic growth was 377 mg/L for phenylalanine, 25 mg/L for tyrosine and 8 mg/L for tryptophan, summing up to 410 mg/L. Hence, the AT-3 strain roughly fixed 725 mg/L of carbon, an amount comparable to that of the control strain, but devoted 56% of the fixed carbon to AAA overproduction.

To produce cinnamic acid and *p*-coumaric acid we expressed the phenylalanine/tyrosine ammonia-lyase XAL from *T. cutaneum* in two different background strains: the AT-3 strain capable of overproducing the respective precursor aromatic amino acid, and a control strain producing wild type levels of aromatic amino acids. Our results show

Table 6
Total concentration of biomass, phenylalanine, tyrosine and tryptophan as well as their respective carbon (C) contents for control and AT-3 strain after 10 days of photoautotrophic growth in BGH11.

		Control		AT-3	
	C %	Total mg/L	C mg/L	Total mg/L	C mg/L
Biomass	49.2	1552	763.58	641	315.37
Phe	65.09	–	–	579.7	376.9
Tyr	59.63	–	–	41.08	24.45
Trp	& 64.7	–	–	12.3	7.96
			Σ 763.58		Σ 724.68

that XAL is highly active in *Synechocystis* and has both phenylalanine and tyrosine ammonia-lyase activity (Table 3). The production of both, cinnamic acid and p-coumaric acid in the X1–3 strains was ~12 fold higher than in the cX control strain indicating the need to overproduce the phenylalanine and tyrosine precursors to achieve high phenylpropanoid production. Overall, after five days of photoautotrophic growth, we measured the production of 470 ± 70.6 mg/gDW of *p*-coumaric acid and 267.2 ± 31.8 mg/gDW of cinnamic acid which correspond to 200.7 ± 30.1 and 114.1 ± 13.6 mg/L of each respective compound in the X3 strain. Both phenylpropanoids were found in the growth medium. To our knowledge this is the highest production of either of those compounds reported for cyanobacteria to date. In *E. coli* expression of XAL resulted in twice as much production of cinnamic acid than *p*-coumaric acid (Vannelli et al., 2007), however in *Synechocystis*, XAL expression resulted in the opposite ratio with twice as much *p*-coumaric acid than cinnamic acid being produced. In the AT-3 strain the carbon allocated for phenylalanine was an order of magnitude higher than the carbon allocated for tyrosine. For example, after five days of photoautotropic growth, AT-3 produced 664 mg/gDW of phenylalanine but only 40.2 mg/gDW of tyrosine. In *Synechocystis* the synthesis of phenylalanine is thought to occur from prephanate via PPN whereas for tyrosine synthesis, prephanate is transaminated to arogenate and then dehydrogenated to tyrosine by $TyrA_a$. Bonner et al. (2004) found $TyrA_a$ activity inhibited by tyrosine whereas Legrand et al. (2006) concluded it is not. Although the mechanism that regulates carbon partitioning through both routes is not known, the difference in phenylalanine and tyrosine production in the AT-3 strain suggests that tyrosine production is a tightly controlled process in *Synechocystis*. Upon introduction of XAL in the AT-3 background we achieved the production of 470 ± 70 mg/gDW of *p*-coumaric acid and only 267 ± 31 mg/gDW of cinnamic acid. The unexpectedly high amount of *p*-coumaric acid produced from tyrosine suggests that tyrosine could act as an allosteric inhibitor for some of its own biosynthetic enzymes because when a tyrosine sink was introduced the flow of carbon from prephanate to *p*-coumaric acid increased 10 times. This supports Bonner et al. (2004) observations regarding the feedback inhibition of $TyrA_a$ by tyrosine. Upon XAL introduction the levels of tyrosine in the X3 strain dropped to 4.5 ± 2.6 mg/gDW. On the other hand, the production of cinnamic acid in the X3 strain was half of what we would expect to see based on previous phenylalanine production in the AT-3 strain. Only 6.4 ± 1.9 mg/gDW of phenylalanine was detected in X3, suggesting that conversion of phenylalanine to cinnamic acid is not the limiting step responsible for low cinnamic acid production. Instead the low amount of cinnamic acid in the X3 strain seems likely due to a 2-fold reduction of carbon allocated to phenylalanine synthesis.

The synthesis of caffeic acid from *p*-coumaric acid is the next step in the phenylpropanoid pathway. Lin and Yan (2012) showed that the native 4- hydroxyphenlacetate 3-hydroxylase complex (HpaBC) from *E. coli* strain W was capable of hydroxylating *p*-coumaric acid to form caffeic acid. The HpaBC complex's large component (HpaB) uses $FADH_2$ as a cosubstrate for hydroxylation, whereas the small component (HpaC) is a NAD(P)H-flavin oxidoreductase that supplies $FADH_2$ to HpaB (Galan et al., 2000; Louie et al., 2003). Because the HpaBC complex catalyzes the self-supply of redox power for its hydroxylase activity we hypothesized that the expression of HpaBC in the AT-3 background could lead to caffeic acid production when combined with XAL. Indeed coexpression of XAL and HpABC in the AT-3 background (XH1-3 strains) resulted in a maximal production of 47.4 ± 13.9 mg/gDW (12.6 ± 3.7 mg/L) of caffeic acid by the XH2 strain after six days of photoautotrophic growth, indicating that HpaBC is active in *Synechocystis*. To our knowledge, this is the highest titer of caffeic acid ever produced in cyanobacteria. However, there is room for improvement as the LC-MS analysis also revealed 161–300 mg/gDW of *p*-coumaric acid left in the XH1–3 strains, suggesting that HpaBC activity is in fact limiting.

3.8. Conclusion and Perspectives

Here we show that introducing the *E. coli* $aroG^{fbr}$ and $tyrA^{fbr}$ genes into *Synechocystis* successfully leads to the overproduction of 904 ± 53 mg/gDW of phenylalanine and 64 ± 3.7 mg/gDW of tyrosine by the AT-3 strain after 10 days of photoautotrophic growth. We estimated that the AT-3 strain invested 56% of the fixed carbon for AAA overproduction. When the XAL enzyme was expressed in the AT-3 background we achieved the total conversion of tyrosine and phenylalanine to 470 ± 70 mg/gDW of *p*-coumaric acid and 267 ± 31 mg/gDW cinnamic acid, respectively. By further introducing the HpaBC enzyme it was possible to produce 47.4 ± 13.9 mg/gDW of caffeic acid. More than 95% of the products were secreted to the growth medium allowing recovery without cell disruption. Future metabolomics and proteomics analysis will help to identify pathway bottlenecks and to further improve titers.

Acknowledgements

The authors acknowledge financial support from the Copenhagen Plant Science Centre, the VILLUM Foundation “Light-driven biosynthesis: Improving photosynthesis by designing and exploring novel electron transfer pathways” (13363), the Novo Nordisk Foundation project “Harnessing the Energy of the Sun for Biomass Conversion” (NNF16OC0021832) and the Carlsberg Foundation (CF17-0657). The authors would also like to thank the Danish National Research Foundation for support of the DynaMo Center (DNRF grant99) and the DynaMo Metabolomics Facility for LC-MS analysis. LFB would like to thank Lisbeth Mikkelsen for maintaining the cyanobacteria strains developed for this work and Lawrence C. Sutardja for his kind assistance to operate the Multi-Cultivator MC 1000-OD.

Appendix A. Supplementary data

Supplementary data to this article can be found online at https://doi.org/10.1016/j.ymben.2019.11.002.

References

Báez-Viveros, J.L., Osuna, J., Hernández-Chávez, G., Soberón, X., Bolívar, F., Gosset, G., 2004. Metabolic engineering and protein directed evolution increase the yield of L-phenylalanine synthesized from glucose in Escherichia coli. Biotechnol. Bioeng. 87 (4), 516–524.

Berla, B.M., Saha, R., Immethun, C.M., Maranas, C.D., Moon, T.S., Pakrasi, H., 2013. Synthetic biology of cyanobacteria: unique challenges and opportunities. Front. Microbiol. 4, 246.

Bonner, C.A., Jensen, R.A., Gander, J.E., Keyhani, N.O., 2004. A core catalytic domain of the TyrA protein family: arogenate dehydrogenase from Synechocystis. Biochem. J. 382 (1), 279–291.

Brown, K., Doy, C., 1966. Control of three isoenzymic 7-phospho-2-oxo-3-deoxy-d-arabino-heptonate-d-erythrose-4-phosphate lyases of Escherichia coli W and derived mutants by repressive and â€œinductiveâ€ effects of the aromatic amino acids. Biochim. Biophys. Acta (BBA) - Enzym. Biol. Oxid. 118 (1), 157–172.

Chang, S.-T., Chen, P.-F., Chang, S.-C., 2001. Antibacterial activity of leaf essential oils and their constituents from Cinnamomum osmophloeum. J. Ethnopharmacol. 77 (1), 123–127.

Chao, C.-y., Mong, M.-c., Chan, K.-c., Yin, M.-c., 2010. Anti-glycative and anti-inflammatory effects of caffeic acid and ellagic acid in kidney of diabetic mice. Mol. Nutr. Food Res. 54 (3), 388–395.

Chemler, J.A., Fowler, Z.L., McHugh, K.P., Koffas, M.A., 2010. Improving NADPH availability for natural product biosynthesis in Escherichia coli by metabolic engineering. Metab. Eng. 12 (2), 96–104.

Chemler, J.A., Koffas, M.A., 2008. Metabolic engineering for plant natural product biosynthesis in microbes. Curr. Opin. Biotechnol. 19 (6), 597–605.

Cheng, S.-S., Liu, J.-Y., Tsai, K.-H., Chen, W.-J., Chang, S.-T., 2004. Chemical composition and mosquito larvicidal activity of essential oils from leaves of different Cinnamomum osmophloeum provenances. J. Agric. Food Chem. 52 (14), 4395–4400.

Chuu, C.-P., Lin, H.-P., Ciaccio, M.F., Kokontis, J.M., Hause, R.J., Hiipakka, R.A., Liao, S., Jones, R.B., 2012. Caffeic acid phenethyl ester suppresses the proliferation of human prostate cancer cells through inhibition of p70S6K and Akt signaling networks. Cancer Prev. Res. 5 (5), 788–797.

Dempo, Y., Ohta, E., Nakayama, Y., Bamba, T., Fukusaki, E., 2014. Molar-based targeted metabolic profiling of cyanobacterial strains with potential for biological production. Metabolites 4 (2), 499–516.

Englund, E., Andersen-Ranberg, J., Miao, R., Hamberger, B., Lindberg, P., 2015. Metabolic engineering of Synechocystis sp. PCC 6803 for production of the plant diterpenoid manoyl oxide. ACS Synth. Biol. 4 (12), 1270–1278.
Entus, R., Poling, M., Herrmann, K.M., 2002. Redox regulation of Arabidopsis 3-deoxy-d-arabino-heptulosonate 7-phosphate synthase. Plant Physiol. 129 (4), 1866–1871.
Galán, B., Díaz, E., Prieto, M.A., García, J.L., 2000. Functional analysis of the small component of the 4-hydroxyphenylacetate 3-monooxygenase of Escherichia coli W: a prototype of a new flavin:NAD(P)H reductase subfamily. J. Bacteriol. 182 (3), 627–636.
Gething, M.-J.H., Davidson, B.E., 1976. Chorismatemutase/prephenate dehydratase from Escherichia coli K12: 2. evidence for identical subunits catalysing the two activities. Eur. J. Biochem. 71 (2), 327–336.
Gibson, D.G., Young, L., Chuang, R.-Y., Venter, J.C., Hutchison III, C.A., Smith, H.O., 2009. Enzymatic assembly of DNA molecules up to several hundred kilobases. Nat. Methods 6 (5), 343.
Guerrero, F., Carbonell, V., Cossu, M., Correddu, D., Jones, P.R., 2012. Ethylene synthesis and regulated expression of recombinant protein in Synechocystis sp. PCC 6803. PLoS One 7 (11), e50470.
Guzman, J.D., 2014. Natural cinnamic acids, synthetic derivatives and hybrids with antimicrobial activity. Molecules 19 (12), 19292–19349.
Hall, G., Flick, M., Gherna, R., Jensen, R., 1982. Biochemical diversity for biosynthesis of aromatic amino acids among the cyanobacteria. J. Bacteriol. 149 (1), 65–78.
Huang, H.-H., Camsund, D., Lindblad, P., Heidorn, T., 2010. Design and characterization of molecular tools for a synthetic biology approach towards developing cyanobacterial biotechnology. Nucleic Acids Res. 38 (8), 2577–2593.
Hussain, M.S., Fareed, S., Saba Ansari, M., Rahman, A., Ahmad, I.Z., Saeed, M., 2012. Current approaches toward production of secondary plant metabolites. J. Pharm. BioAllied Sci. 4 (1), 10.
Jaganathan, S.K., Supriyanto, E., Mandal, M., 2013. Events associated with apoptotic effect of p-coumaric acid in HCT-15 colon cancer cells. World J. Gastroenterol.: WJG 19 (43), 7726.
Jensen, R.A., Nasser, D.S., 1968. Comparative regulation of isoenzymic 3-deoxy-d-arabino-heptulosonate 7-phosphate synthetases in microorganisms. J. Bacteriol. 95 (1), 188–196.
Juminaga, D., Baidoo, E.E., Redding-Johanson, A.M., Batth, T.S., Burd, H., Mukhopadhyay, A., Petzold, C.J., Keasling, J.D., 2012. Modular engineering of L-tyrosine production in Escherichia coli. Appl. Environ. Microbiol. 78 (1), 89–98.
Kaneko, T., Thi, T.H., Shi, D.J., Akashi, M., 2006. Environmentally degradable, high-performance thermoplastics from phenolic phytomonomers. Nat. Mater. 5 (12), 966.
Kikuchi, Y., Tsujimoto, K., Kurahashi, O., 1997. Mutational analysis of the feedback sites of phenylalanine-sensitive 3-deoxy-d-arabino-heptulosonate-7-phosphate synthase of Escherichia coli. Appl. Environ. Microbiol. 63 (2), 761–762.
Landry, B.P., Stöckel, J., Pakrasi, H.B., 2013. Use of degradation tags to control protein levels in the cyanobacterium Synechocystis sp. strain PCC 6803. Appl. Environ. Microbiol. 79 (8), 2833–2835.
Legrand, P., Dumas, R., Seux, M., Rippert, P., Ravelli, R., Ferrer, J.-L., Matringe, M., 2006. Biochemical characterization and crystal structure of Synechocystis arogenate dehydrogenase provide insights into catalytic reaction. Structure 14 (4), 767–776.
Lin, Y., Yan, Y., 2012. Biosynthesis of caffeic acid in Escherichia coli using its endogenous hydroxylase complex. Microb. Cell Factories 11 (1), 42.
Louie, T.M., Xie, X.S., Xun, L., 2003. Coordinated production and utilization of FADH2 by NAD(P)H- flavin oxidoreductase and 4-hydroxyphenylacetate 3-monooxygenase. Biochemistry 42 (24), 7509–7517.
Lütke-Eversloh, T., Stephanopoulos, G., 2005. Feedback inhibition of chorismate mutase/prephenate dehydrogenase (TyrA) of Escherichia coli: generation and characterization of tyrosine-insensitive mutants. Appl. Environ. Microbiol. 71 (11), 7224–7228.
Lütke-Eversloh, T., Stephanopoulos, G., 2007. L-tyrosine production by deregulated strains of Escherichia coli. Appl. Microbiol. Biotechnol. 75 (1), 103–110.
Mir, R., Jallu, S., Singh, T., 2015. The shikimate pathway: review of amino acid sequence, function and three-dimensional structures of the enzymes. Crit. Rev. Microbiol. 41 (2), 172–189.
Mirza, N., Crocoll, C., Olsen, C.E., Halkier, B.A., 2016. Engineering of methionine chain elongation part of glucoraphanin pathway in e. coli. Metab. Eng. 35, 31–37.
Navaneethan, D., Rasool, M., 2014. p-Coumaric acid, a common dietary polyphenol, protects cadmium chloride-induced nephrotoxicity in rats. Ren. Fail. 36 (2), 244–251.
Ogawa, T., Marco, E., Orus, M.I., 1994. A gene (ccmA) required for carboxysome formation in the cyanobacterium Synechocystis sp. strain PCC6803. J. Bacteriol. 176 (8), 2374–2378.
Olson, M.M., Templeton, L.J., Suh, W., Youderian, P., Sariaslani, F.S., Gatenby, A.A., Van Dyk, T.K., 2007. Production of tyrosine from sucrose or glucose achieved by rapid genetic changes to phenylalanine-producing Escherichia coli strains. Appl. Microbiol. Biotechnol. 74 (5), 1031–1040.
Osanai, T., Kanesaki, Y., Nakano, T., Takahashi, H., Asayama, M., Shirai, M., Kanehisa, M., Suzuki, I., Murata, N., Tanaka, K., 2005. Positive regulation of sugar catabolic pathways in the cyanobacterium Synechocystis sp. PCC 6803 by the group 2 σ factor SigE. J. Biol. Chem. 280 (35), 30653–30659.
Osanai, T., Oikawa, A., Azuma, M., Tanaka, K., Saito, K., Hirai, M.Y., Ikeuchi, M., 2011. Genetic engineering of the group 2 sigma factor SigE widely activates the expressions of sugar catabolic genes in Synechocystis sp. PCC 6803. J. Biol. Chem. 286, 30962–30971 jbc–M111.
Patnaik, R., Spitzer, R.G., Liao, J.C., 1995. Pathway engineering for production of aromatics in Escherichia coli: confirmation of stoichiometric analysis by independent modulation of AroG, TktA, and Pps activities. Biotechnol. Bioeng. 46 (4), 361–370.
Pietta, P.-G., 2000. Flavonoids as antioxidants. J. Nat. Prod. 63 (7), 1035–1042.
Pribat, A., Noiriel, A., Morse, A.M., Davis, J.M., Fouquet, R., Loizeau, K., Ravanel, S., Frank, W., Haas, R., Reski, R., et al., 2010. Nonflowering plants possess a unique folate-dependent phenylalanine hydroxylase that is localized in chloroplasts. The Plant Cell 22 (10), 3410–3422.
Rodriguez, A., Martnez, J.A., Flores, N., Escalante, A., Gosset, G., Bolivar, F., 2014. Engineering Escherichia coli to overproduce aromatic amino acids and derived compounds. Microb. Cell Factories 13 (1), 126.
Sakamula, R., Thong-asa, W., 2018. Neuroprotective effect of p-coumaric acid in mice with cerebral ischemia reperfusion injuries. Metab. Brain Dis. 33 (3), 765–773.
Scheepens, A., Bisson, J.-F., Skinner, M., 2014. p-Coumaric acid activates the GABA-A receptor in vitro and is orally anxiolytic in vivo. Phytother Res. 28 (2), 207–211.
Shastri, A.A., Morgan, J.A., 2005. Flux balance analysis of photoautotrophic metabolism. Biotechnology Progress 21 (6), 1617–1626.
Stanier, R., Kunisawa, R., Mandel, M., Cohen-Bazire, G., 1971. Purification and properties of unicellular blue-green algae (order Chroococcales). Bacteriol. Rev. 35 (2), 171.
Vannelli, T., Xue, Z., Breinig, S., Qi, W.W., Sariaslani, F.S., 2007. Functional expression in Escherichia coli of the tyrosine-inducible tyrosine ammonia-lyase enzyme from yeast Trichosporon cutaneum for production of p-hydroxycinnamic acid. Enzym. Microb. Technol. 41 (4), 413–422.
Wlodarczyk, A., Gnanasekaran, T., Nielsen, A.Z., Zulu, N.N., Mellor, S.B., Luckner, M., Thøfner, J.F.B., Olsen, C.E., Mottawie, M.S., Burow, M., et al., 2016. Metabolic engineering of light-driven cytochrome P450 dependent pathways into Synechocystis sp. PCC 6803. Metab. Eng. 33, 1–11.
Wu, S., Chappell, J., 2008. Metabolic engineering of natural products in plants; tools of the trade and challenges for the future. Curr. Opin. Biotechnol. 19 (2), 145–152.
Xue, Y., Zhang, Y., Cheng, D., Daddy, S., He, Q., 2014. Genetically engineering Synechocystis sp. Pasteur Culture Collection 6803 for the sustainable production of the plant secondary metabolite p-coumaric acid. Proc. Natl. Acad. Sci. 111 (26), 9449–9454.
Young, J.D., Shastri, A.A., Stephanopoulos, G., Morgan, J.A., 2011. Mapping photoautotrophic metabolism with isotopically nonstationary 13C flux analysis. Metab. Eng. 13 (6), 656–665.
Zhao, G., Xia, T., Song, J., Jensen, R.A., 1994. Pseudomonas aeruginosa possesses homologues of mammalian phenylalanine hydroxylase and 4 alpha-carbinolamine dehydratase/DCoH as part of a three-component gene cluster. Proc. Natl. Acad. Sci. 91 (4), 1366–1370.